JOURNAL OF SPACECRAFT AND ROCKETS
Vol. 38, No. 3, May–June 2001

Deep Space 1 Measurements of Ion Propulsion Contamination

D. Brinza,* J. Wang,† J. Polk,‡ and M. Henry§
Jet Propulsion Laboratory, California Institute of Technology, Pasadena, California 91109

The first in situ measurements are reported of ion propulsion-induced contamination from an interplanetary spacecraft, NASA's New Millennium Deep Space 1. Deep Space 1 carries two quartz crystal microbalance and calorimeter pairs to characterize contaminant deposition due to ion thruster operation. One pair of sensors has a direct line-of-sight view of the ion engine whereas the other pair is shadowed from direct view of the engine. After about 2750 h of ion thruster operation in the first year of the mission, the line-of-sight sensor has collected about 250 Å of molybdenum, and the non-line-of-sight sensor has only collected the equivalent mass of a 25-Å-thick deposit of molybdenum. The line-of-sight deposition rate appears proportional to the thrust level, whereas the non-line-of-sight deposition rate increases much more rapidly with the thrust level. Measurement results suggest that significant backflow of ionized molybdenum particles would occur primarily at high thrusting levels when both the molybdenum ionization rate and the plume potential relative to the spacecraft are higher than that at lower thrusting levels.

I. Introduction

IT is well understood that ion thruster operation can lead to a variety of spacecraft interactions and contaminations. One may loosely classify ion-propulsion-induced environments as the plasma environment, the contamination environment, and the field environment. The induced-plasma and contamination environments are due to the continued presence of an exhaust plume, which is composed of both the propellant efflux and the nonpropellant efflux. The propellant efflux consists of propellant ions, neutralizing electrons, unionized propellant, and a low-energy charge-exchange plasma generated by the collisions between the fast moving propellant ions and the slow moving neutrals. The nonpropellant efflux comes from the material sputtered from thruster components and the neutralizer. The induced-field environment is primarily due to the static electric and magnetic fields of the thruster and electromagnetic noises generated by the thruster during operation. The interaction of the plasma plume and the ambient plasma environment may also generate electrostatic and electromagnetic fluctuations. Ion-thruster-induced spacecraft–plume interactions have been a subject of extensive experimental and theoretical studies (for example, see Refs. 1–3 and references therein). However, due to a lack of flight opportunities, almost all existing experimental data on ion thruster plume environments are obtained from ground tests of ion thrusters.

NASA's New Millennium Deep Space 1 (DS1), launched on 24 October 1998, is the first interplanetary spacecraft operated on solar electric propulsion. A primary objective of DS1 is to characterize ion-propulsion-induced environments and their effects on spacecraft. DS1 carries a suite of diagnostic sensors designed to provide a comprehensive in-flight investigation of ion-propulsion-induced interactions. These sensors have produced high-quality data. In-flight measurements of the ion propulsion plasma environment and the induced-field environment were reported recently.[4,5] The objective of this paper is to report in-flight observations of ion-propulsion-induced contaminations.

Ground experiments and computational modeling have shown that charge-exchange ions generated within the aperture holes and near the upstream and downstream faces of the accelerator grid can impinge on the grid surface due to its negative bias voltage (see Refs. 6–8 and references therein). Impingement by the charge-exchange ions generated within the grids and downstream will lead to gradual sputtering of the accelerator grid, eventually leading to mechanical failure of the grid structure. The sputtered grid material is ejected primarily as neutral atoms in the general direction of the plume. A fraction of the sputtered particles will also become ionized due to either charge-exchange collisions with the propellant ions or electron impact ionizations. It is well known that both the propellant charge-exchange ions and the ionized sputtered particles can be pushed out of the plume by local electrostatic potential and backflow to interact with spacecraft.

The DS1 thruster uses xenon (Xe), an inert gas, as its propellant. The charge-exchange Xe ions generated within the plume may affect the spacecraft's plasma environment and space plasma measurement performed onboard, but will not cause contamination because Xe is a noncontaminating species. On the other hand, the material of the thruster accelerator grid is molybdenum (Mo). The sputtered Mo species presents a serious contamination hazard due to its low vapor pressure.

In this paper, we analyze the first in situ measurements of the ion-propulsion-induced contamination from an interplanetary spacecraft. The DS1 ion thruster and the contamination diagnostic sensors are described in Sec. II. Data from in-flight measurements are presented in Sec. III. Contaminant deposition rates are discussed and are compared with those obtained from ground measurements in Sec. IV. Section V contains a summary and conclusions.

II. Ion Propulsion Diagnostic Sensors

The flight ion propulsion system (IPS) is developed under the NASA solar electric propulsion technology application readiness (NSTAR) program. The NSTAR ion thruster has a 30 cm diam and is designed to operate over an input power range of 500–2300 W with a thrust of 20–92 mN, a specific impulse of 1950–3100 s, and a total beginning-of-life efficiency of 0.42–0.62. The propellant Xe ions are accelerated through a Mo grid to form a beam with an energy of up to 1100 eV and a current of up to 1.8 A. A detailed description of the NSTAR ion propulsion system and its in-flight validation is given in Ref. 9.

The ion propulsion diagnostic subsystem (IDS) is part of the IPS. IDS is an integrated, comprehensive set of diagnostics designed to characterize ion-propulsion-induced environments and contaminations. IDS has two interconnected hardware units, the diagnostics sensors electronics unit (DSEU) and the remote sensors unit (RSU), and integrates a suit of 12 diagnostic sensors. The contamination and plasma sensors are mounted on the RSU and the field sensors are mounted on the DSEU. The contamination monitors include two quartz crystal microbalance (QCM) and calorimeter (CAL) pairs. The plasma sensors include a retarding potential analyzer, a planar

Received 9 June 2000; revision received 4 December 2000; accepted for publication 20 December 2000.

*Senior Systems Engineer, MS 125-177.
†Principal Member of Engineering Staff; currently Associate Professor, Department of Aerospace and Ocean Engineering, Virginia Polytechnic Institute and State University, Blacksburg, VA 24061-0203. Member AIAA.
‡Supervisor, Advanced Propulsion Technology Group, MS 125-109. Member AIAA.
§Senior Systems Engineer, MS 301-335.

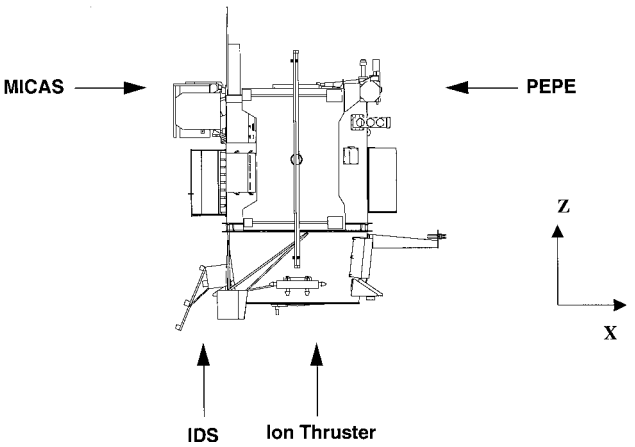

Fig. 1 Deep Space 1 spacecraft.

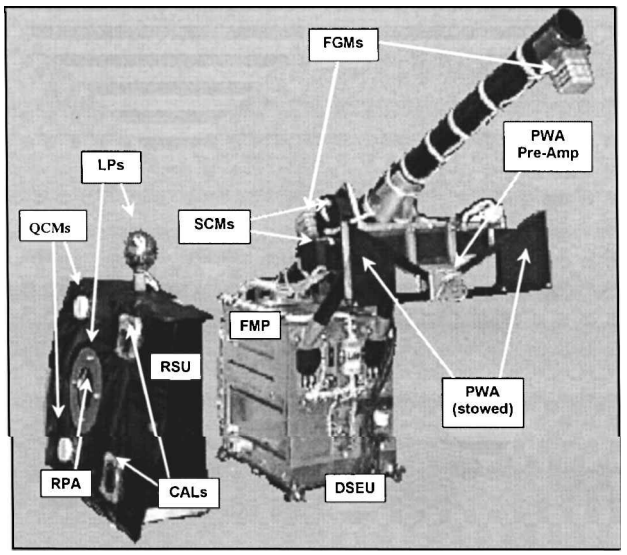

Fig. 2 IDS.

langmuir probe, and a spherical langmuir probe. Electrostatic and electromagnetic noise measurements are made by a plasma wave antenna and a search coil magnetometer. Magnetic field measurements are made by two flux gate magnetometers. Figure 1 shows the DS1 spacecraft. An illustration of the spacecraft with deployed solar arrays is also shown in Ref. 10. Figure 2 shows the IDS instruments.

This paper will focus on in-flight measurements obtained from IDS contamination monitors. The two QCM and CAL pairs are used to characterize mass deposition rates and contamination effects on surface thermooptical properties. The QCMs detect mass variations on the sensor surface via the induced frequency change in the oscillating quartz crystal sensor. The CALs provide information on solar absorptance and hemispherical emittance by temperature measurement of the thermally isolated sensor surface.

The IDS QCM sensors are QCM Research MK16 flight sensors with a fundamental frequency of 10 MHz. The frequency to area mass density conversion is 4.43 ng/cm^2 Hz. Hence, each QCM provides very high-sensitivity measurement (<10 ng/cm^2) of mass accumulation on the sensor.[11] The long-term drift of the QCM should not exceed 50 ng/cm^2/month, which corresponds to a minimum detectable Mo deposit rate of two monolayers per year. The CALs monitor temperature changes and solar illumination of the sense crystal. Each CAL[12] uses the sun as a stimulus for determination of solar absorptance. It also includes a controlled heater to permit measurement of the hemispherical emissivity of the surface. The CAL can determine both solar absorptance changes and emissivity changes to better than 0.01.

The location and orientation of the contamination sensors are shown in Fig. 3. The sensors are located at a distance of 75 cm from the ion thruster beam centerline. One pair of sensors, which will be called QCM0, is oriented to have a direct line-of-sight view

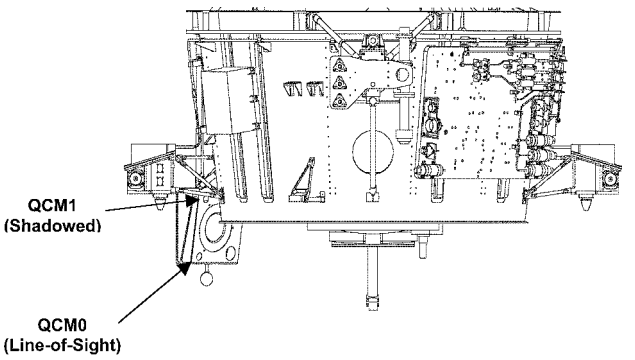

Fig. 3 Close-up of the propulsion module and the location of the contamination sensors.

of the NSTAR ion engine. QCM0 is located 85 deg off of the ion thruster beam centerline. The other pair, which will be called QCM1, is shadowed from direct view of the NSTAR engine by the DS1 propulsion module assembly.

The QCM0 pair is expected to accumulate readily detectable amounts of sputtered Mo. Because only the ionized particles can backflow to reach the non-line-of-sight surfaces,[10] the QCM1 measurements are expected to be dominated by the ionized Mo particles and/or contamination from the spacecraft and launch environments. Hence, the deposition rate on non-line-of-sight surfaces is expected to be low.

III. In-Flight Contamination Measurements

The contamination monitors have functioned properly and have produced high-quality data for assessing the contamination environments on DS1. The data from the QCM and CAL sensors are reduced, analyzed, and correlated with NSTAR ion engine operations. This paper presents data on mass deposition and sensor temperature obtained during the first year of the mission. (Data on solar absorptance changes and emissivity changes will be reported in a subsequent paper.) The results are discussed chronologically in this section. Rates of contamination accumulation during IPS thrusting periods are conveniently expressed in terms of angstroms of Mo per 1000 h of operation: Å/kh.

Because QCM beat frequencies are sensitive to changes in temperature and solar illumination of the sense crystal, temperature changes and solar illumination of the sense crystal affect QCM response. Hence, to extract low-level contamination information, QCM data often must be corrected for temperature and solar illumination. However, we are concerned here with substantial mass accumulation over a long period of time. The magnitude of the IPS-induced contamination for the QCM sensors is such that the corrections for the temperature and solar illumination effects on the QCM measurement are not necessary. Moreover, because Mo is a refractory material, reemission does not occur to Mo, and the accumulation rate is not very sensitive to QCM temperature.

Measurements During Launch Operations

The final preflight functional test of the IDS before launch was conducted on day of year (DOY) 1998-293. Data from the contamination sensors provide the prelaunch baseline for assessing launch-phase contamination in the vicinity of the DS1 to launch vehicle interface. The prelaunch readings, which were obtained in ambient atmosphere at 16°C, were 2475 and 2085 Hz for QCM0 and QCM1, respectively. Following launch, DS1 was oriented such that QCM0 was illuminated with a sun angle of approximately 46 deg, whereas QCM1 is in the shadow of the DS1 propulsion module. The IDS was not activated until 1998-298 at 2201 h (approximately 34 h after launch). The initialization of IDS included a special activity (DFrost) intended to bake off volatile contamination from the QCMs and CAL by heating the sensors to +75°C. Very little change (<50 Hz) was observed in the beat frequency of either QCM as a result of the initial postlaunch DFrost.

The frequencies and temperatures for QCM0 and QCM1 just before DFrost were 2260 Hz (at +30°C) and 2272 Hz (at +16°C),

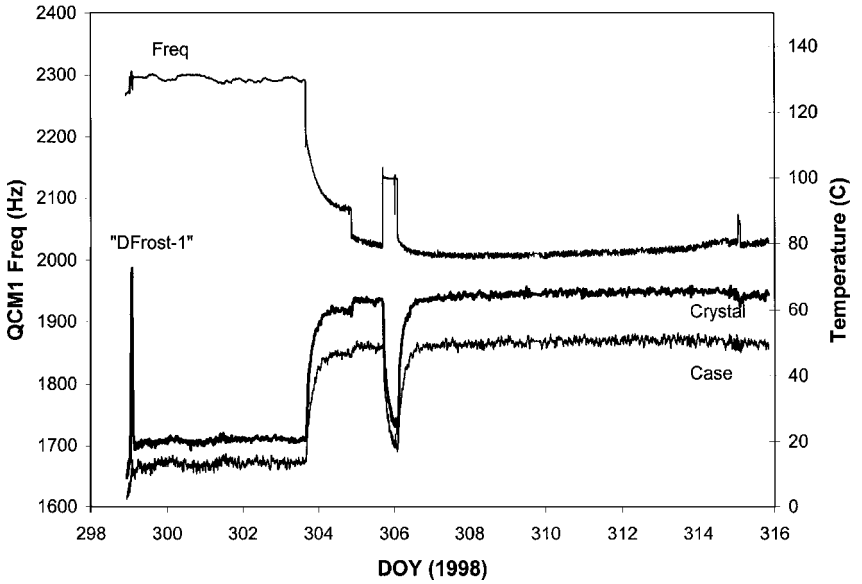

a) QCM1 early mission response

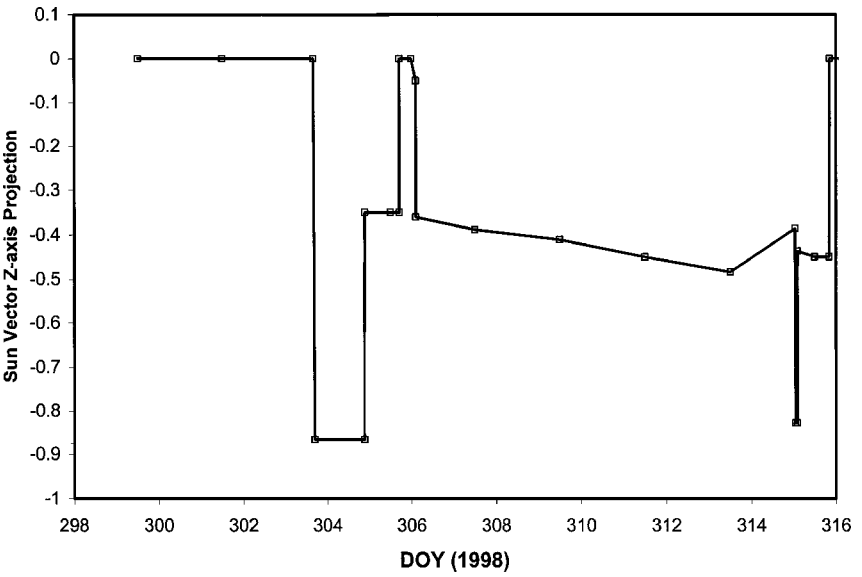

b) Early mission DS1 sun orientation

Fig. 4 QCM1 response and DS1 orientation with respect to the sun during the early phase of the mission (IPS not operating during that period of time).

respectively. Because QCM0 was exposed to the sun after launch, it is suspected that most of the contaminants accumulated on it were evaporated before IDS initialization. The beat frequency for QCM1 increased by 187 Hz from prelaunch to IDS initialization, yielding an estimated 0.8-μg/cm^2 (80-Å) accumulation of organic contamination for the launch phase. This accumulation was not affected by the DFrost activity, but was removed when DS1 rotated to expose the NSTAR ion engine to the sun (NSTAR decontamination maneuver). Figure 4a shows the early mission response of QCM1. The DS1 orientation with respect to the sun is shown in Fig 4b. Note the substantial frequency and temperature changes near DOY 1998-304 associated with the NSTAR decontamination maneuver. There is an additional turn on DOY 1998-305, which further affects the QCM1 frequency and temperature. On DOY 1998-306, DS1 returned to the nominal sun on X-axis orientation. Using the frequency reading at this time, it appears that about a 165-Hz decrease occurred as a result of this solar-stimulated bakeout. Based on this interpretation of QCM1 data, it appears that the RSU surfaces were contaminated with approximately 80 Å of low-volatility organic material, most of which was removed on exposure to the sun.

Measurements During IPS Operations

The QCM data obtained during IPS operations in the first year of the DS1 mission are shown in Figs. 5a–5h. Figures 5a–5h are arranged so that the response of the line-of-sight (QCM0) and non-line-of-sight (QCM1) sensors can be compared side by side. The four pairs of Figs. 5 represent the full time intervals during which IPS operations of substantial duration occurred. Data for minor thrusting events and the trajectory correction maneuvers before the Asteroid Braille encounter do not show significant accumulations on either QCM and are not shown. Similarly, data for the long, nonthrusting intervals are not shown because no accumulation occurred on either QCM in these periods.

To correlate QCM measurements with NSTAR ion engine operations, the NSTAR throttle table is listed in Table 1. In the following discussions, the mission-throttle level (ML) listed in Table 1 will be used in all references to IPS thrusting conditions. To determine the deposition rate for a particular thrust level, a least-squares fit of the frequency data for the time interval containing that ML was performed. The resulting slope in units of hertz per day was then converted to angstroms per 1000 h for Mo by multiplying a unit

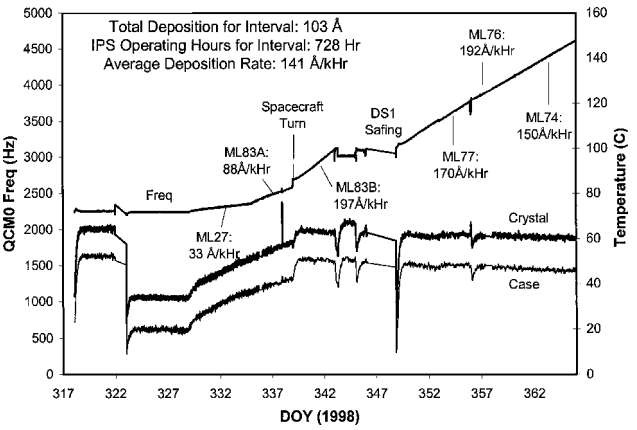

a) QCM0 data for 1998-317-1998-365

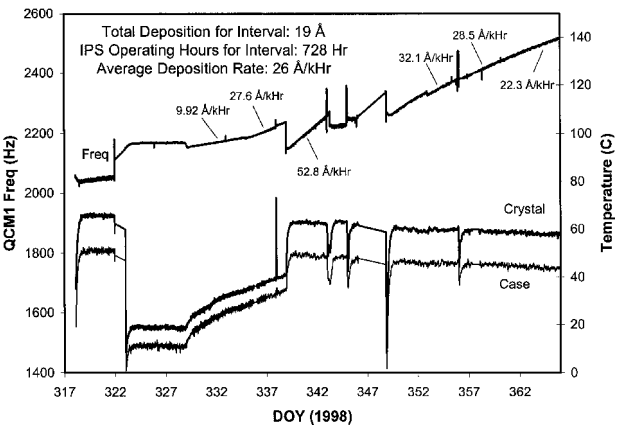

b) QCM1 data for 1998-317-1998-365

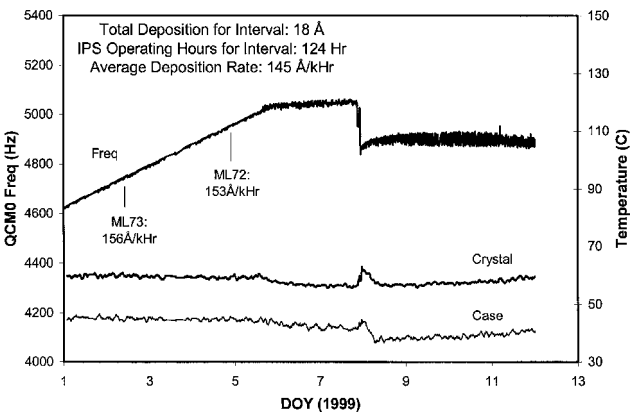

c) QCM0 data for 1999-001-1999-012

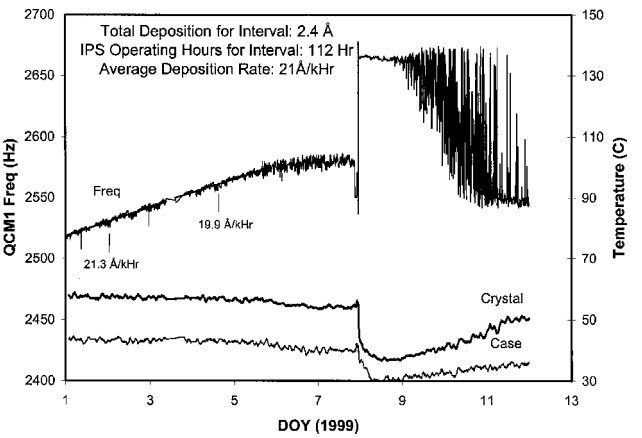

d) QCM1 data for 1999-001-1999-012

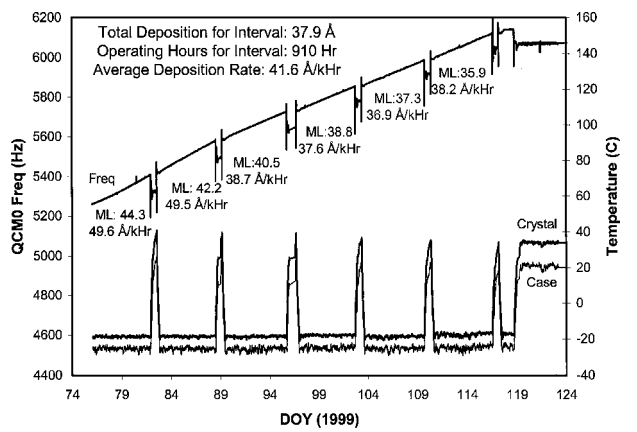

e) QCM0 data for 1999-074-1999-124

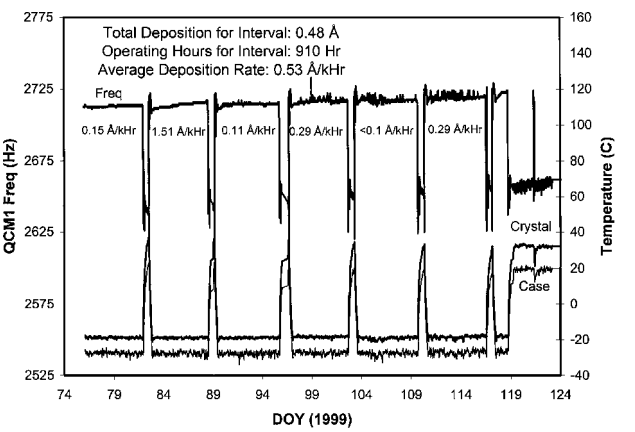

f) QCM1 data for 1999-074-1999-124

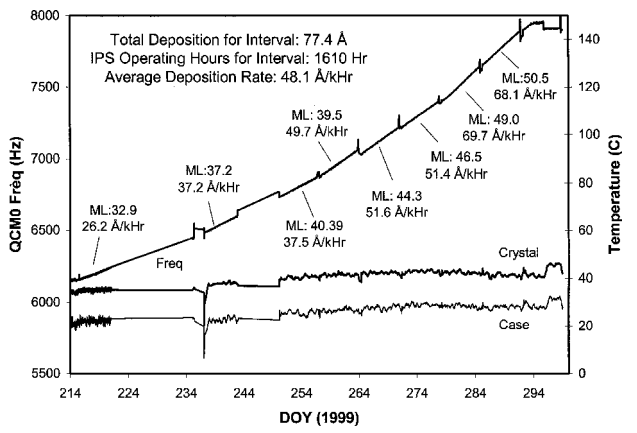

g) QCM0 data for 1999-214-1999-300

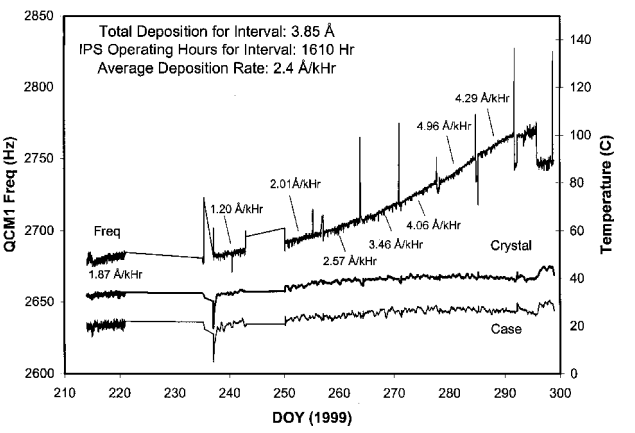

h) QCM1 data for 1999-214-1999-300

Fig. 5 QCM0 and QCM1 data obtained during IPS operations, first year of the mission; frequency data shown on left axis, temperature data shown on right axis. For each thrust segment, the deposition rate is labeled for time-averaged MLs.

Table 1 NSTAR ion thruster flight throttle

NSTAR throttle level	Mission throttle level	PPU input power, kW	Engine input power, kW	Calculated thrust, mN	Main flow rate, sccm	Cathode flow rate, sccm	Neutralizer flow rate, sccm	Specific impulse, s	Total efficiency
15	111	2.52	2.29	92.4	23.43	3.70	3.59	3120	0.618
14	104	2.38	2.17	87.6	22.19	3.35	3.25	3157	0.624
13	97	2.25	2.06	82.9	20.95	3.06	2.97	3185	0.630
12	90	2.11	1.94	78.2	19.86	2.89	2.80	3174	0.628
11	83	1.98	1.82	73.4	18.51	2.72	2.64	3189	0.631
10	76	1.84	1.70	68.2	17.22	2.56	2.48	3177	0.626
9	69	1.70	1.57	63.0	15.98	2.47	2.39	3136	0.618
8	62	1.56	1.44	57.8	14.41	2.47	2.39	3109	0.611
7	55	1.44	1.33	52.5	12.90	2.47	2.39	3067	0.596
6	48	1.32	1.21	47.7	11.33	2.47	2.39	3058	0.590
5	41	1.19	1.09	42.5	9.82	2.47	2.39	3002	0.574
4	34	1.06	0.97	37.2	8.30	2.47	2.39	2935	0.554
3	27	0.93	0.85	32.0	6.85	2.47	2.39	2836	0.527
2	20	0.81	0.74	27.4	5.77	2.47	2.39	2671	0.487
1	13	0.67	0.60	24.5	5.82	2.47	2.39	2376	0.472
0	6	0.53	0.47	20.6	5.98	2.47	2.39	1972	0.420

conversion factor of 1.804. The deposition rates are labeled in Fig. 5 for time-averaged ML for each thrust segment.

The first period of extended IPS operations occurred from DOY 1998-328 to DOY 1999-005. The line-of-sight sensor (QCM0) response is shown in Figs. 5a and 5c, whereas the shadowed sensor (QCM1) response is seen in Figs. 5b and 5d. The initial IPS operations consisted of 10 days thrusting with the thrust vector essentially Earth pointed. During these initial operations, the NSTAR engine was first operated at low thrust (ML 6–ML 27) for five days. During this period, QCM0 frequency increased by 123 Hz while QCM1 frequency increased by 25 Hz.

QCM0 data for the remaining thrusting of the initial period show some interesting features. On DOY 1998-338, DS1 performed a turn to orient the thrust vector from Earth pointed to the desired mission trajectory thrust attitude. Note that the Mo deposition rate for QCM0 at ML 83 before DOY 1998-338 was 88 Å/kh, whereas after the turn, the deposition rate increased to 197 Å/kh. It is speculated that this rate change is due to thermal distortion effects on the NSTAR ion engine grids. There have been no reports of change in mass sensitivity with varying sun angle on QCMs, and so the rate change is not considered to be an instrument artifact.

Following the turn to thrust attitude, DS1 continued thrusting until DOY 1998-342. Other technology activities, including initial turn on of the plasma experiment for planetary exploration (PEPE) instrument were performed. On DOY 1998-346, IPS was restarted at a low-thrust level (ML 6) to assess the effects of IPS operation on the PEPE instrument. The onboard sequence raised the IPS thrust level to ML 85 after 15 min. The available power for IPS thrusting was overestimated, resulting in a DS1 safe-mode transition. IPS thrusting resumed on DOY 1998-348 after DS1 spent 2 days in safe mode.

The first IPS thrust segment ended with 2 weeks of essentially continuous thrusting with the thrust levels gradually decreasing from ML 78 on DOY 1998-352 to ML 72 on DOY 1999-005. During this interval, the DS1 onboard navigation software would update the thrust vector and level at 12-h intervals. The IPS thruster was turned off at 1600 h on DOY 1999-005. The deposition on QCM0 steadily increased over this interval, except for a brief period on DOY 1998-356 when DS1 reoriented to place the sun on the X axis for approximately 3 h. QCM1 also showed consistent frequency increase, although an order-of-magnitude lower than that for QCM0. The thrust segment continued into early 1999. Steady accumulation by both QCMs is shown in Figs. 5c and 5d. Subsequent to engine turn off on DOY 1999-005, DS1 performed maneuvers to characterize the effects of stray light into the miniature integrated camera and spectrometer (MICAS) imager. The $\mathcal{O}(100)$ Hz oscillations from DOY 1999-009 through DOY 1999-012 in Fig. 5d are caused by minor sun-angle changes on QCM1 during these maneuvers.

The next major IPS thrust interval was from DOY 1999-075 until DOY 1999-117. This thrusting was performed with weekly optical navigation (OpNav) activities and high-rate telemetry downlink intervals. The thrusting duty cycle was typically greater than 90% during this interval. The OpNav/downlink events are readily identified in Figs. 5e and 5f by 100-Hz frequency dips in both QCM0 and QCM1, as well as 60°C temperature increases for both sensors. During this period, the onboard navigator commanded the desired IPS thrust level. The DS1 power management software would monitor battery state of charge and perform thrust reduction as required. For this period, the non-line-of-sight sensor accumulated only about 1% of the amount of Mo collected by QCM0.

Subsequent to the Asteroid Braille encounter on DOY 1999-210, IPS operated for an interval of almost 12 weeks. As the DS1 sun distance decreased, the thrust level gradually increased. The deposition rates of both QCMs also increased during this period, as seen in Figs. 5g and 5h. The brief, periodic spikes in the QCM frequency data occur at each of the weekly OpNav and downlink sessions, again caused by sun-angle changes. The accumulation of Mo on the shadowed QCM is about 5% of that witnessed by the line-of-sight sensor.

The four thrusting segments shown in Figs. 5a–5h account for over 95% of the IPS operating time for the first year of the mission. Of the 250 Å of Mo collected on the line-of-sight QCM0 in the first year of operation, almost 95% of the accumulation is shown in Figs. 5a–5h. The shadowed QCM1 only collected the equivalent mass of a 25-Å-thick deposit of Mo in the first year, or approximately 10% of the Mo deposited on QCM0. The source of this non-line-of-sight contaminant is attributed to ionized Mo moving along trajectories affected by electrostatic potentials associated with the thruster plume and spacecraft surfaces.[10] However, it is possible that a portion of the deposited mass on the shadowed QCM1 is not Mo, perhaps from general spacecraft outgassing contamination.

IV. Discussion

Deposition Dependence on Thrust Level

The deposition rate averaged over the entire IPS operating time for the first year of the mission is 90 Å/kh for QCM0 and about 9 Å/kh for QCM1, respectively. However, the deposition rate differs significantly at different thrust levels. The deposition rates for QCM0 and QCM1 averaged for each thrusting segment are summarized in Fig. 6 as a function of ML. Deposition data collected during the first 10 days of IPS operation are not included in Fig. 6 because the thruster had a sun angle very different from that during the rest thrusting segments (the thrust vector is essentially Earth pointed during the first 10 days) and the QCM temperature changed significantly during that period. Most of the thrustings were performed at ML 32–ML 45. A few thrusting segments were performed at ML 74–ML 83. Note that the accelerator grid voltage is at −150 V for thrusting levels below ML 56 and at −180 V for thrusting levels above ML 56. Because of the IPS operations profile, there are no data available

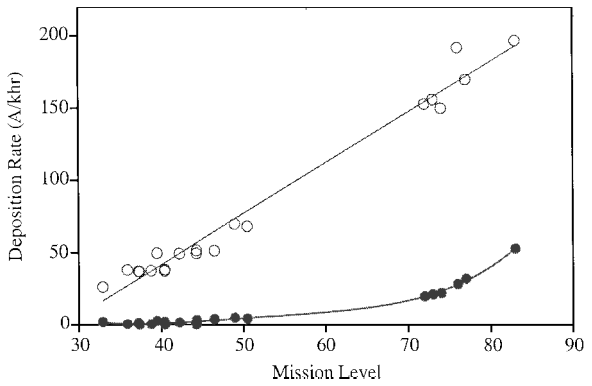

Fig. 6 QCM0 and QCM1 deposition rate vs ML.

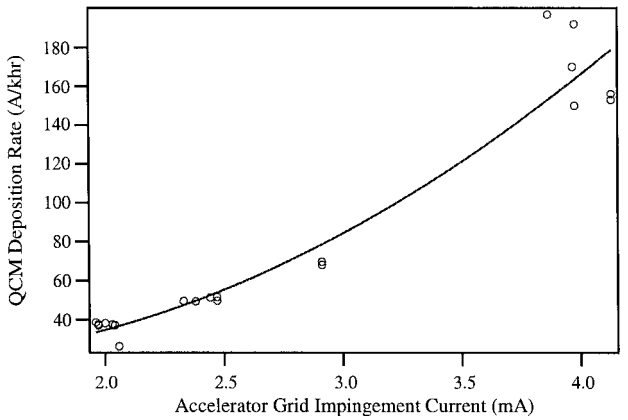

Fig. 7 QCM0 deposition rate vs grid impingement current.

for thrust levels from ML 50 to ML 70. As already discussed, the line-of-sight QCM0 accumulates Mo at a substantially higher rate than the shadowed QCM1. The line-of-sight sensor deposition rate appears roughly proportional to the thrust level, whereas the non-line-of-sight rate increases much more rapidly with thrust levels.

We next examine the deposition rate against two important parameters associated with IPS operation, the beam current and the accelerator grid impingement current. The beam current and the impingement current at different thrust levels are obtained from engine flight data.[9]

The amount of the sputtered Mo particles is directly related to grid erosion, which in turn is caused by ion impingement on the accelerator grid. In Fig. 7, we plot the QCM0 deposition rate as a function of the measured accelerator grid impingement current. Figure 7 shows a linear relationship between the deposition rate and the impingement current at low- and midthrottle levels, which is expected. However, deposition rates at the higher throttle levels (with impingement currents of about 4 mA) appear to deviate from this trend. One explaination for this is that these data were measured early in the flight, and the erosion rate may have been higher than at later times because of direct ion impingement. Direct impingement of beam ions at an energy of 1100 eV on portions of the accelerator grid may occur early in the operation of an engine. As these parts of the aperture walls are eroded away, the direct impingement decreases, and the erosion is dominated by charge-exchange ions.

Deposition at the non-line-of-sight QCM1 is primarily due to the ionized Mo particles, which can backflow toward the upstream region of the thruster exit under the influence of the local electric field. The electric field is a function of the space charge from the ion beam.[4,10] Hence, in Fig. 8, we plot the QCM1 deposition rate as a function of the ion beam current. Similar to Fig. 6, Fig. 8 shows that deposition at QCM1 increases at a much higher rate at higher beam currents that is, higher thrust levels. We offer the following arguments to explain this observation. First, the production of the ionized Mo particles is expected to increase significantly at higher thrust levels for the following reasons: 1) More sputtered molybdenum atoms are produced due to increased grid impingement by charge-exchange ions. 2) More beam ions are produced by the engine, increasing the rate for charge-exchange ionization of Mo atoms. 3) Higher electron temperatures are observed at higher thrust levels,[4] increasing the rate for electron impact ionization of Mo atom. Second, more ionized molybdenum particles will be able to backflow toward the upstream region because the potential difference between the plume and the spacecraft increases significantly as the beam current increases. For instance, in-flight measurements show that the plume potential relative to spacecraft is about 15 V at ML 83 (beam current 1.40 A), whereas it is about 9 V at ML 36 (beam current 0.82 A) (Ref. 4).

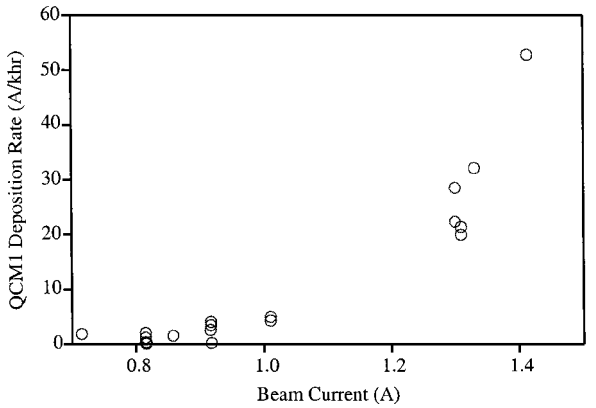

Fig. 8 QCM1 deposition rate vs beam current.

Comparison with Ground-Test Results

It is also interesting to compare in-flight measurements with measurements obtained in a ground-test environment. The NSTAR 8000-h life demonstration test (LDT) performed at the Jet Propulsion Laboratory afforded the opportunity to measure the thickness and composition of deposits accumulated from extended ion engine operation on ground.

The LDT contamination monitors were mounted on a curved support beam at 120 cm from the engine and were placed at angles from 40 to 110 deg from the thrust axis at 10-deg intervals. To avoid collection of sputtered chamber material, the witness windows were placed in 25-cm-long tubes lined with tantalum foil. At the entrance of the tube, a collimating aperture was positioned to limit the witness field of view to the ion engine grid. Recall that, on DS1, the line-of-sight QCM0 is located at 75 cm from the thruster centerline, 85 deg off thrust axis.

During LDT, the NSTAR ion engine was operated at the full power, 2.5 kW, for 8000 h. At the end of LDT, the Mo deposition at the 85 deg off thrust axis position is found to be about 500 Å, and the average deposition rate is about 62.5 Å/kh. Even though the grid is an extended source, the deposition thickness is roughly inversely proportional to square of distance from grids. Hence, the expected deposition rate for an LDT witness monitor in the equivalent position of the line-of-sight QCM0 is 160 Å/kh. This result is comparable to the in-flight QCM0 deposition rate for high mission levels (see Fig. 6).

V. Conclusions

For the first time, a comprehensive in-flight investigation of ion-propulsion-induced contamination is carried out on an interplanetary spacecraft. The IDS on DS1 has obtained high-quality contamination measurements. The results are useful from two perspectives. First, the in-flight data provide information to characterize the contamination environment for future spacecraft using ion propulsion. Second, the data, when correlated with ground test, can help assess ion engine health because contamination measurements can provide an indication of grid wear.

After about 2750 h of IPS operation in the first year of the DS1 mission, the line-of-sight QCM0 has collected about 250 Å of Mo and the non-line-of-sight QCM1 has only collected the equivalent mass of a 25-Å-thick deposit of Mo. The line-of-sight QCM0 deposition rate appears proportional to the mission level, ranging

from about 33 Å/kh at ML 27 to about 200 Å/kh at ML 83. The QCM0 deposition rate is consistent with ground measurements obtained during the NSTAR ion thruster 8000-h life test. The non-line-of-sight QCM1 rate exhibits a nonlinear behavior, increasing much more rapidly with thrust levels. The primary source of the non-line-of-sight contaminant is attributed to ionized Mo. QCM1 results suggest that significant backflow of ionized Mo particles will occur only at high thrusting levels when both the Mo ionization rate and the plume potential relative to the spacecraft are higher than that at lower thrusting levels. Because the DS1 solar arrays do not extend into the line-of-sight zone, are well removed from the thruster (>2 m), and are negatively grounded, the amount of Mo deposited on the solar concentrator arrays with linear element technology (SCARLET) concentrator lenses is expected to be very small.

Acknowledgments

This work was performed at Jet Propulsion Laboratory (JPL), California Institute of Technology, under a contract with NASA, and was supported by the NASA New Millennium Deep Space 1 (DS1) mission and the NASA Solar Electric Propulsion Technology Application Readiness (NSTAR) project. We acknowledge technical support provided by the DS1 mission and the NSTAR project. We acknowledge many helpful discussions with O. Duchemin and J. Brophy (JPL), I. Katz (Maxwell Laboratories), and R. Samanta Roy (Institute of Defense Analysis).

References

[1]Carruth, M. (ed.), "Experimental and Analytical Evaluation of Ion Thruster/Spacecraft Interactions," Jet Propulsion Lab., Publication 80-92, California Inst. of Technology, Pasadena, CA, 1981.

[2]Samanta Roy, R., Hastings, D., and Gatsonis, N., "Numerical Study of Spacecraft Contamination and Interactions by Ion-Thruster Effluents," *Journal of Spacecraft and Rockets*, Vol. 33, No. 4, 1996, pp. 535–542.

[3]Wang, J., Brophy, J., and Brinza, D., "Three-Dimensional Simulations of NSTAR Ion Thruster Plasma Environment," AIAA Paper 96-3202, July 1996.

[4]Wang, J., Brinza, D., Young, D., Nordholt, J., Polk, J., Henry, M., Goldstein, R., Hanley, J., Lawrence, D., and Shappirio, M., "Deep Space One Investigations of Ion Propulsion Plasma Environment," *Journal of Spacecraft and Rockets*, Vol. 37, No. 5, 2000, pp. 545–555.

[5]Henry, M., Brinza, D., Mactutis, A., McCarty, K., Rademacher, J., vanZandt, T., Johnson, R., Musmann, G., and Kunke, F., "NSTAR Diagnostic Package Architecture and Deep Space One Spacecraft Event Detection," Inst. of Electrial and Electronics Engineers, IEEE Conf. Paper 11.0502, March 2000.

[6]Peng, X., Ruyten, W., and Keefer, D., "Charge-Exchange Grid Erosion Study for Ground-based and Space-based Operations of Ion Thrusters," International Electronic Propulsion Conf., IEPC Paper 93-173, Sept. 1993.

[7]Polk, J., Anderson, J., Brophy, J., Rawlin, V., Patterson, M., Sovey, J., and Hamley, J., "An Overview of the Results from an 8200 Hour Wear Test of the NSTAR Ion Thruster," AIAA Paper 99-2446, 1999.

[8]Crofton, M., and Boyd, I., "The Origins of Accelerator Grid Current: Analysis of T5-Grid Test Results," AIAA Paper 99-2443, 1999.

[9]Polk, J., Kakuda, R., Anderson, J., Brophy, J., Rawlin, V., Patterson, M., Sovey, J., and Hamley, J., "Validation of the NSTAR Ion Propulsion System on the Deep Space One Mission: Overview and Initial Results," AIAA Paper 99-2274, June 1999.

[10]Wang, J., Brinza, D., and Young, M., "Three-Dimensional Particle Simulations of Ion Propulsion Plasma Environment for Deep Space 1," *Journal of Spacecraft and Rockets*, Vol. 38, No. 3, 2001, pp. 433–440.

[11]Wallace, D., and Wallace, A., "Realistic Performance Specifications for Flight Quartz Crystal Microbalance Instruments for Contamination Measurement on Spacecraft," AIAA Paper 88-2727, 1988.

[12]Reichardt, P., and Triolo, J., "Preflight Testing of the ATS-1 Thermal Coatings Experiment," *Thermophysics of Spacecraft and Planetary Bodies*, Progress in Astronautics and Aeronautics, Vol. 20, Academic Press, New York, 1967, pp. 491–513.

I. D. Boyd
Associate Editor